External pH Effects on the Depolarization-activated K Channels in Guard Cell Protoplasts of *Vicia faba*

NITZA ILAN,* AMNON SCHWARTZ,* and NAVA MORAN‡

From the *Department of Agricultural Botany, Faculty of Agriculture, the Hebrew University of Jerusalem Rehovot 76100; and ‡Department of Neurobiology, Weizmann Institute of Science, Rehovot 76100 Israel

ABSTRACT Previous studies reveal that the pH of the apoplastic solution in the guard cell walls may vary between 7.2 and 5.1 in closed and open stomata, respectively. During these aperture and pH changes, massive K^+ fluxes cross the cellular plasma membrane driving the osmotic turgor and volume changes of guard cells. Therefore, we examined the effect of extracellular pH on the depolarization-activated K channels (K_D channels), which constitute the K^+ efflux pathway, in the plasma membrane of *Vicia faba* guard cell protoplasts. We used patch clamp, both in whole cells as well as in excised outside-out membrane patches.

Approximately 500 K_D channels, at least, could be activated by depolarization in one protoplast (density: $\sim 0.6\ \mu m^{-2}$). Acidification from pH 8.1 to 4.4 decreased markedly the whole-cell conductance, G_K, of the K_D channels, shifted its voltage dependence, G_K-E_M, to the right on the voltage axis, slowed the rate of activation and increased the rate of deactivation, whereas the single channel conductance was not affected significantly. Based on the G_K-E_M shifts, the estimated average negative surface charge spacing near the K_D channel is 39 Å. To quantify the effects of protons on the rates of transitions between the hypothesized conformational states of the channels, we fitted the experimental macroscopic steady state conductance-voltage relationship and the voltage dependence of time constants of activation and deactivation, simultaneously, with a sequential three-state model CCO. In terms of this model, protonation affects the voltage-dependent properties via a decrease in localized, rather than homogeneous, surface charge sensed by the gating moieties. In terms of either the CO or CCO model, the protonation of a site with a pK_a of 4.8 decreases the voltage-independent number of channels, N, that are available for activation by depolarization.

INTRODUCTION

The stomata in plants constantly change their aperture controlling leaf gas exchange. Opening of stomata results from uptake of K^+, Cl^-, and malate sythesis, followed by osmotic water influx, increase in turgor and guard cells swelling (MacRobbie, 1987;

Address correspondence to N. Moran, Department of Neurobiology, Yaglom Building, Weizmann Institute, Rehovot, 76100 Israel.

J. GEN. PHYSIOL. © The Rockefeller University Press · 0022-1295/94/05/0807/25 $2.00
Volume 103 May 1994 807–831

Outlaw, 1983). The driving force for these fluxes is proton extrusion by the H^+ pump in the plasma membrane, which hyperpolarizes the cell and acidifies the extracellular millieu (Raschke and Humble, 1973; Spanswick, 1981; Zeiger, 1983; Assmann, Simoncini, and Schroeder, 1985; Shimazaki, Iino, and Zeiger, 1986). Stomatal closure may be initiated by cessation of H^+ extrusion, followed by loss of ions, mainly Cl^- and K^+, osmotic water efflux, and reduction of guard cell turgor. During this cyclic proton pump operation, apoplastic pH may vary between 7.2 and 5.1, as documented using fluorescence methods and H^+-sensitive electrodes (Edwards, Smith, and Bowling, 1988). Similar variation of apoplastic pH was determined also in another type of motor cells, pulvinar extensor cells, with H^+-sensitive electrodes (Lee and Satter, 1989; Starrach and Mayer, 1989).

K channels appear to serve as the pathway for K^+ movement through the guard cell plasma membrane: K^+ enters the swelling cell via hyperpolarization-activated K channels (K_H, or K_{in} channels) and leaves the shrinking cell via depolarization-activated K channel (K_D or K_{out} channels) (Schroeder, Raschke, and Neher, 1987; Schroeder, 1988).

K_H and K_D channels are the most predominant K channel types in the plasma membrane of protoplasts from stomatal guard cells of *Vicia faba* (Hedrich and Schroeder, 1989), and, in fact, in most higher plant cells examined so far (Moran, Ehrenstein, Iwasa, Bare, and Mischke, 1986; Moran, Ehrenstein, Iwasa, Mischke, and Satter, 1988; Moran and Satter, 1989; Schauf and Wilson, 1987; Ketchum, Shrier, and Poole, 1989; see recent reviews by Tester, 1990; Blatt, 1991). The characterization of these channels in plants still lags behind their counterparts in animal cell membranes (see, for example, recent reviews by Sanders, 1990, Hille, 1992) in biophysical as well as in biochemical detail. For example, we are not aware of any information on the density of negative surface charges near the ion channels in plant cell membranes. There are only very few attempts at modeling of channel gating in plants (Bertl, Klieber, and Gradmann, 1988; Sanders, 1990; Schroeder, 1989; Blatt, 1991, 1992; Van Duijn, 1993). When available, gating parameter estimates can serve as a reference for quantitative comparison with data from other systems. Such comparison becomes increasingly important especially now, with the appearance of cloned and reconstituted variants of the K channels from plants (outward rectifier: Cao, Anderova, Crawford, and Schroeder, 1992; inward rectifier: Anderson, Huprikar, Kochian, Lucas, and Gaber, 1992; Schachtman, Schroeder, Lucas, Anderson, and Gaber, 1992; Sentenac, Bonneaud, Minet, Lacroute, Salmon, Gaymard, and Grignon, 1992). Our description of the gating and the external pH effects extends the characterization of K_D channels in guard cell protoplasts.

In animal cells, cation-selective channels are frequently blocked by extracellular protons (Woodhull, 1973; Hille, 1973; Huang, Catterall, and Ehrenstein, 1978; Hagiwara, Miazaki, Moody, and Patlak, 1978; Begenisich and Danko, 1983), with the apparent pK_a of ~ 5. In contrast, a similar H^+ concentration activated sodium channels in one reported case (Ueno, Nakaye, and Akaike, 1992), and chloride channels in another (Hanke and Miller, 1983). Since in the case of the guard cell, pH values ranging from 5 to 7.5 are of physiological significance, we set out to examine the effect of extracellular pH on the K_D channels in guard cell protoplasts isolated from *Vicia faba* leaves. To this end we combined macroscopic steady state and kinetics

data and also single-channel data. The description of gating, based on the macroscopic kinetics of the K_D channels required a minimum of three states: $Closed_1$-$Closed_2$-Open. Therefore, we used the framework of the three-state model and described the effect of pH on the gating of these channels in terms of the Eyring rate theory, i.e., in terms of the transitions between their conformational states. Preliminary reports have appeared in an abstract form (Ilan, Schwartz, and Moran, 1991, 1992).

MATERIALS AND METHODS

Experimental Methods

Plant material. Seeds of *Vicia faba* (supplied by Amir Co., Tel Aviv, Israel) were sown in 12-cm diameter drained pots in a mixture of standard compost and basalt gravel (4:1 by volume) and were watered twice daily with 50% Hogland's nutrient solution and tap water, alternately. The plants were grown in the Phytotron of the Faculty of Agriculture in Rehovot, in glass-covered growth rooms under natural sunlight (70–75% of outdoor levels) extended to 16-h photoperiod with 75 W incandescent lamps (5 $\mu mol \cdot m^{-2} \cdot s^{-1}$ at plant level). Temperature was kept at 22°C during the day (hours 0800–1600) and 17°C at night. Atmospheric humidity was maintained at a constant vapor pressure of 1.2 kPa. The youngest, fully expanded leaves of 3–4 wk-old plants were harvested. Protoplasts were isolated according to procedure of Kruse, Tallman, and Zeiger (1989). We measured the diameters of the spherical protoplasts using a microscope micrometer with a resolution of 0.22 μm (at a magnification of 400). The average diameter of the globular guard cell protoplast was 16.6 ± 1.2 μm (mean ± SD, n = 122), and the calculated average cell surface was 865 ± 125 μm^2.

Electrophysiology. The patch-clamp technique is described in detail by Hamill, Marty, Neher, Sakmann, and Sigworth (1981). The application to plant cell protoplasts is described in detail by Moran et al. (1988), and by Moran, Fox, and Satter (1990). Briefly, a drop of the protoplast suspension was added to ~200 μl of the recording solution, the protoplasts were allowed to settle and stick to the glass bottom of the recording chamber and then washed with ~2–3 ml of the recording solution. The patch pipette was then brought into contact with the protoplast and a whole cell configuration was attained, to be followed, in some experiments, by excision of an outside-out patch.

All experiments were performed in a voltage-clamp mode, using the Axopatch C-1 amplifier (Axon Instruments, Inc., Foster City, CA), and were under computer control, using a software-hardware system from Axon Instruments (Pclamp program package and the TL1-1-125 Labmaster DMA A/D and D/A peripherals).

Membrane potential was controlled according to a preprogrammed schedule, and the resulting membrane current was filtered at 20–100 Hz (−3 db, 4-pole Bessel filter), sampled at 200–500 Hz and stored for further analysis. The error in voltage clamping of the whole cell membrane, largely due to the access resistance, R_s, of the patch pipette was compensated at ~70% by analog circuitry of the Axopatch amplifier. R_s values were ~30 ± 8 MΩ (mean ± SD, n = 27), whereas the resistance of the cells ranged between 4 ± 2 GΩ (mean ± SD, n = 27) at rest (determined from leak current, see below) and 194 ± 46 MΩ (mean + SD, n = 6) measured at peak activity (based on G_K at 63 mV at pH 8.1). The average capacitance was 8.9 ± 0.2 pF (mean ± SD, n = 25). This permits the calculation of specific capacitance: 1.03 ± 0.03 $\mu F \cdot cm^{-2}$ (mean ± SD, n = 25). The measured membrane potential was corrected for liquid-junction potential determined separately using the experimental solutions and 3 M KCl-filled agar bridges (−17 mV).

Solutions. The intracellular solution in the patch pipette contained (in micromolar): 100 glutamate, 105 K^+, 6 Mg^{2+}, 4 Cl^-, 0.2 BAPTA (estimated free $[Ca^{2+}]_i < 10^{-7}$ M), 4 ATP, 20 HEPES, pH 7.2, and manitol, to final osmolarity of 520 mOsm. Due to the effectively infinite increase of the cytoplasm volume in the whole-cell configuration and to the fast equilibration of small solutes in this combined pipette-cell compartment (Marty and Neher, 1983), the interior of the cell is clamped at pH 7.2, and the pH changes affect only the external cell surface. The control bath solutions contained 11 K^+, 1 Ca^{2+}, 2 Mg^{2+}, 6 Cl^-, 10 glutamate, 10 MES, pH 5.5. Bath solution for pH 4.4 included 100 MES, rather than 10, or 7 glutamate and 10 MES (we did not observe any differences between the two subgroups); for pH 7 and 8 it included 10 HEPES, rather than MES; and, in addition, 1.25 and 7.5 of *N*-methylglucamine (NMG), respectively. Solutions with other pH values contained intermediate concentrations of NMG. Final osmolarity of all bath solutions was adjusted with mannitol to 480 mOsm. BAPTA-K_4 was from Molecular Probes, Inc. (Eugene, OR). Mannitol was from Merck. All other chemicals were from Sigma Chemical Co. (St. Louis, MO).

Theoretical Considerations

Initial data reduction. First, we obtained the whole-cell steady state and instantaneous I_M-E_M (current-voltage) relationships. Due to the delay in channel activation, the instantaneous current (leak) could be determined at the beginning of a depolarizing step from the resting potential. The isochronal (usually: steady state) K_D channel current values, I_M, were obtained by subtracting this leak current from the current measured at the end of a 5-s voltage pulse. Then, the steady state G_K-E_M (chord conductance–membrane potential) relationship was extracted from I_M-E_M using Eq. 1:

$$G_K = I_M/(E_M - E_{rev}), \tag{1}$$

where E_{rev} is the reversal potential (Hodgkin and Huxley, 1952) of this current. Whenever tested, the instantaneous I_M-E_M relationship was linear over the examined E_M range, which justifies the use of Eq. 1 for the calculation of G_K.

Analogously, E_{rev} and the single channel conductance, γs, were estimated from the single-channel current, I_s-E_M relationship in outside-out patches. This was obtained either directly, in a response to a ramp-voltage commands, or from the amplitude histograms of steady state current records at various E_M.

In addition, we described the kinetics of current activation and of current deactivation in terms of time constants (τ's) vs E_M. We obtained these τ's by fitting current relaxations with two (activation) or one (deactivation) exponential term(s).

Modeling: an overview. We used the macroscopic steady state whole-cell data for most of our analyses, examining separately the effect of pH on voltage-independent, and the voltage-dependent properties. The information about kinetics was integrated with that about steady state in the modeling of the voltage-dependent K_D channel gating.

We used single-channel data, mainly to obtain directly the single channel conductance and, in addition, for comparison with channel gating in whole cells.

It is important to emphasize that due to the scatter of the pooled data, we did not attempt to compare and choose among different models (except when fitting the activation time courses). We did, however, use several widely accepted general models (see below) and based on these, we extracted estimates of models' parameters. Our only claim is that these parameters are unique.

Boltzmann distribution. The voltage dependence of the steady state G_K resides in the probability for the K_D channel to be open, P_0:

$$G_K = G_{max} \cdot P_o, \tag{2}$$

where G_{max} is the voltage-independent maximum value of G_K. Assuming an equilibrium distribution of the K_D channels between a closed and an open state, and replacing the voltage-dependent P_0 with a simple Boltzman equation:

$$P_o = 1/(1 + e^{-zF(E_M-E_o)/RT}), \tag{3}$$

where E_0 is the half-activation voltage, z is the number of effective charges transfered upon activation, R is the universal gas constant, F is the Faraday constant and T is the absolute temperature, we fitted the individual steady state G_K-E_M relationships for each cell and pH with the combined equation:

$$G_K = G_{max}/(1 + e^{-zF(E_M-E_o)/RT}) \tag{4}$$

The resulting values of G_{max} and E_0 were used in subsequent analyses.

Henderson-Hasselbalch relationship for G_{max}. By definition, G_{max} is voltage independent. We assumed, instead, that G_{max} increases as the fraction of the nonprotonated form of the K_D channel, and that only one site undergoes protonation. Therefore, we fitted the mean G_{max}-pH data determined between pH 8.1 and 4.4 with the Henderson-Hasselbalch relationship:

$$G_{max} = G'/(1 + 10^{pK_a-pH}), \tag{5}$$

where G′ is the maximum conductance in proton absence and pK_a is the pH at which half of the sites are protonated. Because G_{max} is composed of N, the number of available channels in the membrane, and γ_s, the single channel conductance:

$$G_{max} = N \cdot \gamma_S, \tag{6}$$

an effect on either one of them could underlie the effect on G_{max}.

Surface charge. E_0 characterizes the voltage-dependent gating. We assumed that the shift of E_0 with acidification results from the titration of negative charges at the external surface of the membrane in the vicinity of the K_D channel (Gilbert and Ehrenstein, 1969, 1970), and fitted the E_0-pH relationship with the Grahame equation (Grahame, 1947):

$$\sigma^2 = G^{-2} \sum_i c_i(e^{-z_iF(B-E_o)/RT} - 1) \tag{7}$$

modified to include proton binding (Gilbert and Ehrenstein, 1969, 1970):

$$\sigma^2 = \sigma_t^2 \left(1 + \frac{[H^+]_o}{K_{sc}} e^{-F(B-E_o)/RT}\right)^{-2}, \tag{8}$$

where σ is the negative surface charge density, σ_t is the total density of the titratable negative charges, c_i are the concentrations of various ions in the medium, z_i are their respective valencies, K_{sc} is the dissociation constant of the protons from the negative surface charges, $[H^+]_0$ is the proton concentration in the bulk solution, G is a constant equal to 264 (Å/electronic charge) · (mol/liter)$^{1/2}$ at 23°C, and B is the surface potential at the pH (5.5) at which the shift of E_0 is defined as 0 mV. The actual parameters fitted were: d_t (σ_t^{-2}), pK_{sc} (=−log (K_{sc}) and B.

Binomial distribution. We assumed that there are N available independent and identical channels in a patch, with a voltage-dependent P_0 probability to be open. Their product yields the average number of open channels, $\bar{n}$:

$$\bar{n} = N \cdot P_o. \tag{9}$$

To extract P_0 and N separately, we fitted the binomial distribution:

$$P_r = \frac{N!}{r!(N-r)!} P_o^r (1 - P_o)^{(N-r)} \qquad r = 0, 1, \ldots N, \tag{10}$$

to single channel data, where P_r is the probability that r channels will be open simultaneously. Experimentally, P_r is given by the relative weight of the r^{th} peak in an amplitude histogram of a single-channel current record (Iwasa, Ehrenstein, Moran, and Jia, 1986).

The CCO model. According to this model, the K_D channel undergoes the following transitions:

$$\text{Closed}_1 \underset{\delta}{\overset{\gamma}{\leftrightarrow}} \text{Closed}_2 \underset{\beta}{\overset{\alpha}{\leftrightarrow}} \text{Open}$$

where α, β, γ, δ denote the rate constants of transitions between the neighboring states.

We hypothesized that these rate constants are exponential functions of membrane potential (Hodgkin and Huxley, 1952; Ehrenstein, Blumenthal, Latorre, and Lecar, 1974):

$$\begin{aligned} \alpha &= B_2 e^{A_{20}(E_M - E_2)F/RT}, \\ \beta &= B_2 e^{-A_{02}(E_M - E_2)F/RT}, \\ \gamma &= B_1 e^{A_{12}(E_M - E_1)F/RT}, \\ \delta &= B_1 e^{-A_{21}(E_M - E_1)F/RT}, \end{aligned} \tag{11}$$

where E_M is the membrane potential, A_{21} and A_{12}, are the effective charges moved (number of elementary charges × distance of movement) back and forth, respectively, upon transitions $C_1 \leftrightarrow C_2$, A_{02}, and A_{20} are the effective charges moved back and forth upon transitions $C_2 \leftrightarrow O$, E_1, and E_2 are membrane potentials at which the rates of transitions ($C_1 \leftrightarrow C_2$ and $C_2 \leftrightarrow O$, respectively) in opposite directions between the neighboring states are equal and B_1 and B_2 are the values of rates at E_1 or E_2, respectively. In a three-state model, the time constants of current relaxations upon step changes of membrane potential, are complicated combinations of the transition rate constants (Huang, Moran, and Ehrenstein, 1984):

$$\tau_{1,2} = \frac{2}{\alpha + \beta + \gamma + \delta \pm \sqrt{(\alpha + \beta + \gamma + \delta)^2 - 4(\alpha\gamma + \beta\gamma + \beta\delta)}} \tag{12}$$

In steady state conditions, the probability P_0 for a three-state channel to be in an open (conducting) state is given by:

$$P_o = \frac{1}{1 + \beta/\alpha(1 + \delta/\gamma)} \tag{13}$$

or, with the ratios β/α and δ/γ replaced by two Boltzmann distributions governing the population of the three states (Behrens, Oberhauser, Bezanilla and Latorre, 1989):

$$P_o = \frac{1}{1 + e^{-z_2 F(E_M - E_2)/RT}(1 + e^{-z_1 F(E_M - E_1)/RT})} \tag{14}$$

where z_1 and z_2, are the effective charges moved upon transitions $C_1 \leftrightarrow C_2$ and $C_2 \leftrightarrow O$, i.e., the respective sums (in pairs) of A_{21} and A_{12}, and of A_{02} and A_{20}.

Thus, within the framework of the three-state model, eight parameters and a scaling factor (see below) are required for the quantitative description of both the steady state conductance

and the conductance relaxation kinetics, as a function of membrane potential. These parameters can be extracted by a simultaneous fit of equations 11–14, i.e., τ_1, τ_2 and P_0, vs E_M, to the experimental data.

Details of analysis and fitting. Nemst potentials were calculated from ion concentrations using activity coefficients from Appendices 8.9 and 9.10 from Robinson and Stokes (1965). Initial data reduction was performed with the Pclamp software (Axon Instruments, Inc.).

Mean ± SD were used to indicate range of variability. However, when comparison between means was intended, ±SEM was used. When errors of estimated parameters were given, n signified the number of points used for the fit.

Eq. 4 was fitted to individual G_K-E_M relationships using the 386-Matlab program subroutines from Mathworks, Inc. (Natick, MA), implementing the Nelder-Meade simplex algorithm for error minimization.

For the fitting of Eq. 5 to mean G_{max} values, we used NLIN, the nonlinear regression routine of SAS (Statistical Analysis System, ver. 5) from SAS Institute Inc. (Cary, NC) implementing least mean squares minimization.

The same routine of SAS was also used to fit Eq. 10 (with the constraint that N, the number of channels in the patch, be integer) to the observed distribution of probabilities, P_r, of multiple channel openings in a patch, minimizing the χ^2 (the sum, over all combinations of multiple openings, of $\{[P_{r(observed)} - P_{r(calculated)}]^2/P_{r(calculated)}\}$).

To extract the surface charge model parameters, we combined the Eqs. 7 and 8 into a polynomial, derived the roots from the coefficients of the polynomial for each experimental value of pH, and minimized the difference between the observed E_0 (mean values) and that calculated from the larger of the two positive solutions of the polynomial (see also Becchetti, Arcangeli, Del Bene, Olivotto, and Wanke, 1992). To find the polynome roots, we used the Fortran subroutine C02AGF from the commercially available NAG library (from the National Algorithm Group, United Kingdom; releases 14 and 15). The fitting routines were Fortran implementation of unconstrained combined Gauss-Newton and modified Newton algorithm for error minimization (Gill and Murray, 1978), subroutine E04FDF.

For the simultaneous fitting of the CCO model (Eqs. 11–14) we used also the Fortran NAG subroutine E04FDF. While the calculations and fits of the CCO model were performed with the pooled, not averaged, data, for presentation in the figures the normalized values of τ's and G_K's were averaged over several cells.

To minimize variability among cells, especially important when fitting models to data, G_K values at all pH's were normalized to G_{max} at pH 5.5 for the same cell, the values of E_0 for each cell and pH were expressed as shifts relative to E_0 at pH 5.5, and the values of the two activation time constants (τ_1 and τ_2) and the single deactivation time constant (τ_d) were normalized to the maximum value of τ for each cell, and at each pH (which, for the CCO model, is equivalent to the scaling of all four rate constants by the same factor; see Eqs. 11 and 12).

When fitting data with models, several starting guesses for the parameters were tried, to avoid entrapment in a local minimum. The weighing factor used in the fit was equal to the inverse of the standard deviation (when fitting means), calculated separately at each value of E_M. To evaluate goodness of fit we calculated $R' = 1 - S_{res}/S_{tot}$, where S_{res} is the sum of squared vertical deviations of data from the model predictions, and S_{tot} is the sum of squared vertical deviations of data points from the mean. $R' = 1$ means perfect fit to the model, $R' = 0$ means that the model is no better than a straight horizontal line drawn through the mean (SYSTAT, version 1992, from SYSTAT Inc., Evanston, Ill). In the case of binomial distribution, we evaluated the goodness of fit using the standard χ^2 table (Draber, Schultze, and Hansen, 1993), and N (maximum number of synchronous openings used in the calculation of χ^2) degrees of freedom. The number of total non-correlated observations was estimated, roughly, as the ratio

of the total length of the record to the longest time constant of gating observed (Draber et al., 1993).

RESULTS

Proton Block of Macroscopic K_D Channel Currents and Conductance

Depolarization of whole-cell membrane above −30 mV elicited outward currents, whose magnitude was proportional to the amplitude of the depolarizing step (Fig. 1). As shown by others (Schroeder et al., 1987; Schroeder, 1988, Assmann, Moran, and Schwartz, 1988), these currents are carried through a ubiquitous type of K channels, the depolarization-activated K channels, which we will term here the K_D (corresponding to the K_{out} of Schroeder [1988]). The lower the pH of the external medium, the

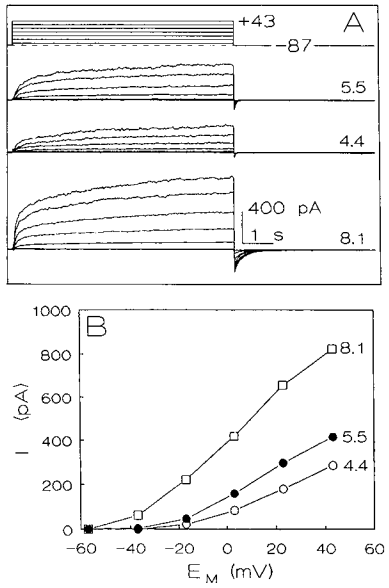

FIGURE 1. Depolarization and time dependence of K currents at pH 5.5, 4.4 and 8.1. (*A*) *Top*, voltage pulses protocol; *bottom*, time course of current relaxations (superimposed separately at each pH) elicited by the voltage pulses. The interval between the pulses was 20 s. Note the changes in the magnitude of currents and in the rates of activation and deactivation. Note also the reversibility of the effect of acidification. (*B*) Current-voltage (*I–V*) relationship of *A* at the indicated pH values: pH 8.1 (□), 5.5 (●), and 4.4 (○).

smaller were the depolarization-activated outward currents. This effect was fully reversible (Fig. 1). The reversal potential (E_{rev}, Hodgkin and Huxley, 1952) of these current was −41.8 ± 0.5 mV (mean ± SEM, n = 8, Fig. 2). For comparison, E_{rev} for the hyperpolarization-activated K channels (K_{in}, Schroeder [1988]) in the same experiments was −52.0 ± 1.1 mV (n = 10, data not shown, but see also Schroeder [1988]). Both E_{rev} values are close to the calculated Nernst potential of K^+ in the experimental solutions, −54 mV (the Nernst potentials of the three other permeant ions in the solutions, Ca^{2+}, H^+ and Cl^- were, respectively, ≥200 mV (with internal $[Ca^{2+}]$ buffered at $<10^{-7}$ M), +100 and −10 mV).

While pH changes did not affect the reversal potential (Fig. 2), the whole-cell steady state K_D channel conductance, G_K (Eq. 1), was diminished by acidification (Figs. 2 *B* and 3 *A*). On average, G_K decreased by ~75% with acidification between 8.1 and 4.4 (Fig. 3 *A*).

Fig. 3 *B* depicts the dual effect of acidification on K_D channels kinetics: an increase of the $t_{1/2}$ of activation (the half activation time) at 63 mV (*full circles*), and a decrease of the deactivation time constant, τ_d, at −87 mV (*empty circles;* the deactivating, tail, currents could be approximated well with a single exponential; data not shown, but see Schroeder [1989]). The slowing down of activation and the speeding up of deactivation are consistent with the blocking effect of protons.

The Effect of Protons on the Steady State Properties of G_K

To learn how the steady state activation of the K_D channel by depolarization is altered by external protons, we fitted the steady state G_K-E_M relationships at the various pH's with the Boltzmann distribution (Eq. 4; Fig. 3 *A, solid lines*). The voltage-independent

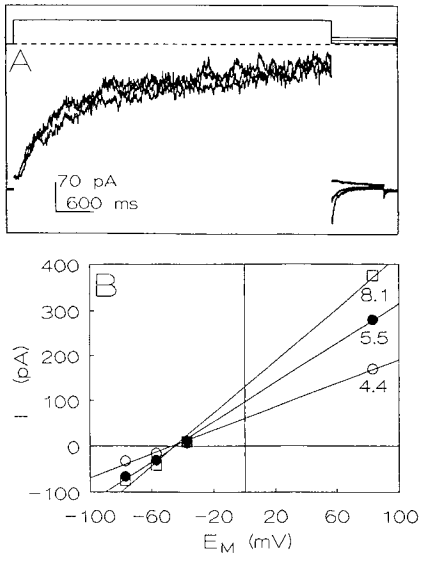

FIGURE 2. Determination of E_{rev} and G_K at various pH values. (*A*) Two-pulse voltage protocol (*top*) elicited whole-cell membrane currents (superimposed, *bottom*); the membrane potential was repeatedly stepped, for 5 s, from the holding potential of −87 to 83 mV, then, in turn, to each of the following: −77, −57, and −37 mV. The interval between the pairs of pulses was 13 s. (*B*) Instantaneous I_M-E_M relationship at pH 8.1 (□), 5.5 (●) and 4.4 (○). (*Lines*) Linear regression to data (*symbols*) at each pH. Note the linearity of this relationship over the entire voltage range. In this particular cell, the slope (G_K) changed with acidification from pH 8.1 to 4.4 from 2.9 ± 0.1 nS, through 2.2 ± 0.1 nS (at pH 5.5) to 1.3 ± 0.1 nS, respectively. The respective reversal potential values were: −45.7 ± 8.1, −44.6 ± 3.8, and −47.5 ± 7.5 mV.

maximum conductance, G_{max}, as well as the half-activation voltage, E_0, were both altered by external pH (Fig. 4, *A* and *B*). The average value of G_{max} at pH 5.5 was 2.6 ± 1.1 (mean ± SD, n = 27). The (normalized; see Materials and Methods) values of G_{max} could be related to pH by the Henderson-Hasselbalch equation (Eq. 5, Fig. 4 *A, solid line*), with a pK_a of 4.8 ± 0.3 (±estimated error, n = 6). If the G_{max} values of pH 8.1 were excluded from the fit, the resulting pK_a was 4.6 ± 0.1 (n = 5; Fig. 4 *A, dashed line*).

The average E_0 at pH 5.5 was 7.7 ± 8.2 mV (mean ± SD, n = 27). Fig. 4 *B* illustrates the shift, relative to pH 5.5, of the average E_0 with pH. Fitting this E_0 shift vs pH with the modified Grahame equation (Eqs. 7 and 8, Fig. 4 *B, line*), yielded the following properties (best fit values) of the assumed negative charges at the external

surface of the membrane in the vicinity of the K_D channel: the average charge separation, d_t = 39 ± 12 Å, the pH at which half of the charges are protonated, pK_{sc} = 4.8 ± 0.6 and the surface potential at pH 5.5, B = −20 ± 13 mV.

In contrast to the change in E_0, the average values of z at the different pH's did not vary significantly and their mean was 1.6 ± 0.4 (mean ± SD, n = 54; Fig. 4 *C*).

The Effect of pH on Single K_D Channels

In all excised outside-out patches, we recorded several, usually identical, channels. Their identification as K_D channels was based (*a*) on the value of the reversal potential and (*b*) on the dependence of their activation on depolarization above the

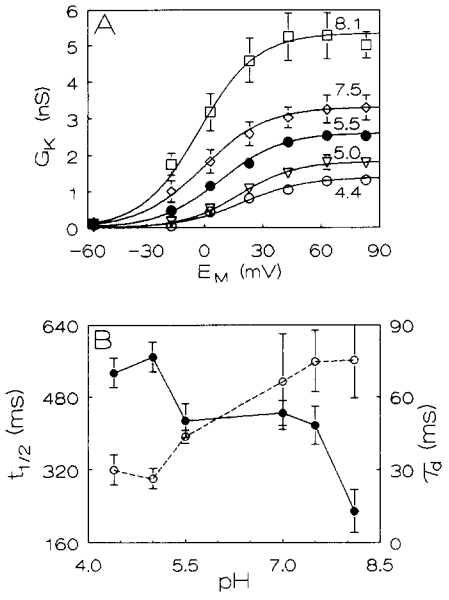

FIGURE 3. pH effects on macroscopic K conductance. (*A*) Average chord conductance, G_K (±SEM), obtained using Eq. 1, vs E_M, at the indicated pH values: 4.4 (○, n = 7), 5.0 (▽, n = 5), 5.5 (●, n = 27), 7.5 (◇, n = 5), 8.1 (□, n = 6). G_K-E_M at pH 7.0 (n = 4; ommitted for clarity) was same as at pH 7.5. The normalized G_K values (see Materials and Methods) were rescaled back to absolute values using the average G_{max} of pH 5.5 of 2.6 nS. (*Lines*) Calculated from Eq. 4, using the averaged best-fit parameters determined at each pH, as in Figs. 4, *A–C*. Cells different from those of Fig. 1. (*B*) Average $t_{1/2}$ (±SEM) of activation vs pH at a depolarization step of 63 mV (●) and average time constant of deactivation, τ_d, vs pH at a holding potential of −87 mV (○). Note the opposite effect of pH. From the same data as in Fig. 3 *A*.

reversal potential (Figs. 5, 6), and more specifically, (*c*) on the same voltage sensitivity as that of macroscopic currents, as reflected in the effective number of gating charges, z = 2 (as in Fig. 4 *C*).

To characterize the voltage dependence of the single K_D channels, as a first approximation a simple Boltzman distribution was fitted to the voltage dependence of the average number of open channels, $\bar{n}$, in one patch at pH 5.5 (Fig. 6 *D*). The effective number of gating charges was at least 2 (1.7 ± 0.4; ± estimated error). The voltage for half activation was 34 ± 4 mV (± estimated error). This is significantly larger than the average E_0 value of 7.7 ± 1.6 mV (mean ± SEM, n = 27) determined in whole cells at pH 5.5 (Fig. 4 *B*). We were disappointed to find, however, that in 9 out of 11 outside-out patches at pH 5.5 that we examined, $\bar{n}$ fluctuated markedly throughout the experiment (even with records lasting 200 s, with over 1,600 opening

events per record) which precluded the determination of these parameters. A dependence of $\bar{n}$ on depolarization was evident, however, between two ranges of E_M: −17 to +3 mV, vs. 23 to 43 mV, when the differences between $\bar{n}$ obtained individually at each E_M, were averaged at each E_M range separately. On average, $\bar{n}$ at the higher depolarization range was 0.60 ± 0.12 (mean ± SEM; n = 10), which was significantly larger—by 0.21 ± 0.07 ($P < 0.01$, single-tailed paired t test) than $\bar{n}$ at the lower depolarization range.

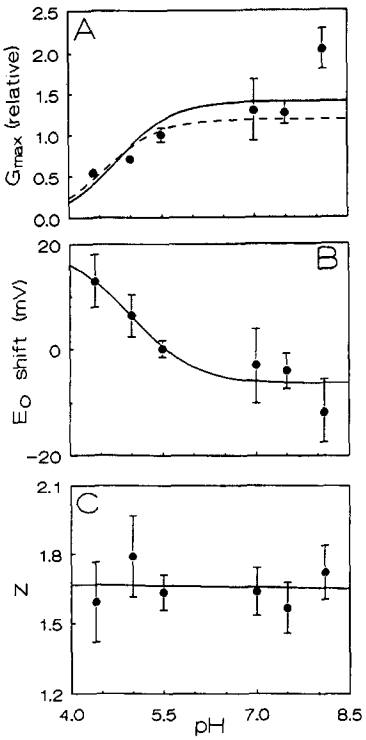

FIGURE 4. pH dependence of the parameters of steady state G_K-E_M relationships. The following are averages (±SEM) of best-fit parameters extracted from individual G_K-E relationships at each pH separately, from data of Fig. 3. Where not visible, the error bars are smaller than the symbol sign. (*A*) The maximum, voltage-independent conductance, G_{max}, normalized to G_{max} at pH 5.5 (average G_{max} at pH 5.5 is 2.6 ± 0.2 nS (±SEM, n = 27); the error bars at pH 5.5 are SEM of G_{max} before normalization). Continuous line represents a fit, with SD^{-1} as weights, of Eq. 5 in pH range 4.4–8.1, to the mean values of G_{max} with best fit values: pKa = 4.81 ± 0.31 and G′ = 1.41 ± 0.19 (±estimated error; n = 6, R′ = 0.647). Dashed line: the data at pH 8.1 excluded from the fit. pKa = 4.61 + 0.14 and G′ = 1.19 + 0.08 (±estimated error; n = 5, R′ = 0.889). (*B*) The midpoint of activation, E_o, relative to E_0 at pH 5.5 (average absolute value of E_0 at 5.5: 7.7 ± 1.6 mV (±SEM, n = 27; this is indicated by the error bars at pH 5.5). (*Line*) Fit of Eqs. 4 and 5, with SD^{-1} as weights, to the mean data points, with best fit parameters: average negative surface charge spacing, $(\sigma_l)^{-2}$ = 39 ± 12 Å, pK_{sc} 4.8 ± 0.6, and B = −20 ± 13 mV (±standard error estimate, n = 6; R′ = 0.889). (*C*) The effective charge transfered upon channel opening, z. Line: linear regression to points, R′ = 0.06. Note the lack of pH effect on z. Average z = 1.65 + 0.10 (±SEM, n = 54).

In spite of the fluctuations of $\bar{n}$ (e.g., Fig. 6 *D*, at pH 4.4), we observed a (reversible!) decrease of channel activity due to acidification. In Fig. 5 *A*, predominantly 1 channel appeared to be active at pH 5.5. In contrast, two channels became clearly active during the voltage ramp at pH 8.1 (Fig. 5 *B*). A similar tendency during alkalinization from 5.5 to 8.1 was observed also in another patch (not shown). Acidification from pH 5.5 to 4.4 reduced single channel activity in two additional outside-out patches (e.g., Fig. 6). On average (irrespective of E_M), in these two

patches, $\bar{n}$ decreased significantly, by 0.66 ± 0.22 (±SEM, $P < 0.01$, 11 determinations), at E_M ranging from −17 to 83 mV. To resolve this decline in channel activity into a separate effect on either N or P_0 (Eq. 9), we fitted the distribution of probabilities of the multi channel openings in these patches to the binomial distribution (Eq. 10, illustrated in Figs. 6, *E* and *F*). In spite of the fluctuation observed in both N and P_0 (not shown), in the above two patches N decreased significantly from 4.4 ± 0.3 (±SEM), by 2.0 ± 0.3 ($P < 0.005$), while the average change in P_0 was not significantly different from zero (−0.04 ± 0.03; $P < 0.30$, two-sided paired t test). We have not studied systematically the fluctuations in $\bar{n}$ to decide on a possible underlying mechanism, such as shifts between various modes of gating and cooperativity among the channels (e.g., Draber et al., 1993, Iwasa et al., 1986). The elucidation of these phenomena requires additional experiments.

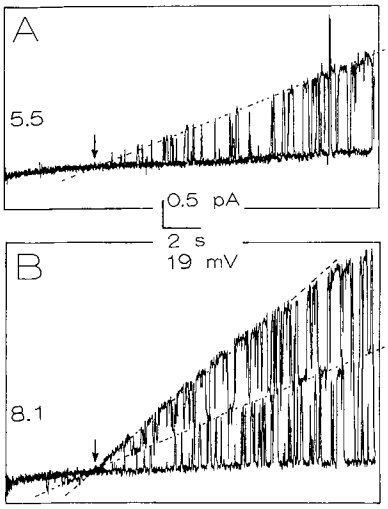

FIGURE 5. The effect of pH between 5.5 and 8.1 on single K_D channels in an outside-out patch. Single channel current (two superimposed traces in each panel) during slow voltage ramps from the holding potential of −87 mV to 103 mV. Upward deflection indicate channel opening and outward current. Dashed lines (fitted by eye) mark the increasing amplitude of the single channel current. Compare the linearity of the single-channel current-voltage relationship with that of the instantaneous I_M-E_M relationship in the whole cell (Fig. 2 *B*). Note that the I-E_M relationship of the single channel current changed very little during pH change from 5.5 (*A*) to 8.1 (*B*). γs changed from 12.6 to 14.5 to pS and E_{rev} (*arrows*) remained constant at −43 mV. Also note that predominantly one channel was open at pH 5.5 and two channels were frequently open simultaneously at pH 8.1. Data filtered at 20 Hz, and sampled at 100 Hz.

In contrast to the irregularity of $\bar{n}$, the values of E_{rev} and the single channel conductance, γs, were fairly constant at pH 5.5, during each experiment and from patch to patch. E_{rev} of the single-channel currents was identical to that of the whole cell currents (−42.0 ± 2.7 mV (SEM, $n = 7$); two examples are depicted in Figs. 5 and 6). As in whole-cell measurements, pH change did not change E_{rev} significantly (Figs. 5 and 6 *C*). Neither did it significantly alter γ_s. The average γ_s at pH 5.5 was 10 ± 2 pS (SD; $n = 7$). All the following changes were within the 95% confidence interval of the mean of γ_s at pH 5.5. In two patches, γ_s at pH 5.5 was lower, roughly by 15%, than at pH 8.1 (12.6 pS vs 14.5 pS, respectively; Fig. 5, *A* and *B*), or by 8% (12.6 pS vs 13.6; not shown). In two additional patches, acidification from 5.5 to 4.4 increased γs by ~15%, from 9.1 to 10.5 pS (Fig. 6 *C*), or decreased γ_s by 4%, from 12.0 to 11.5 pS (not shown). Thus, if the single channel conductance was similarly pH

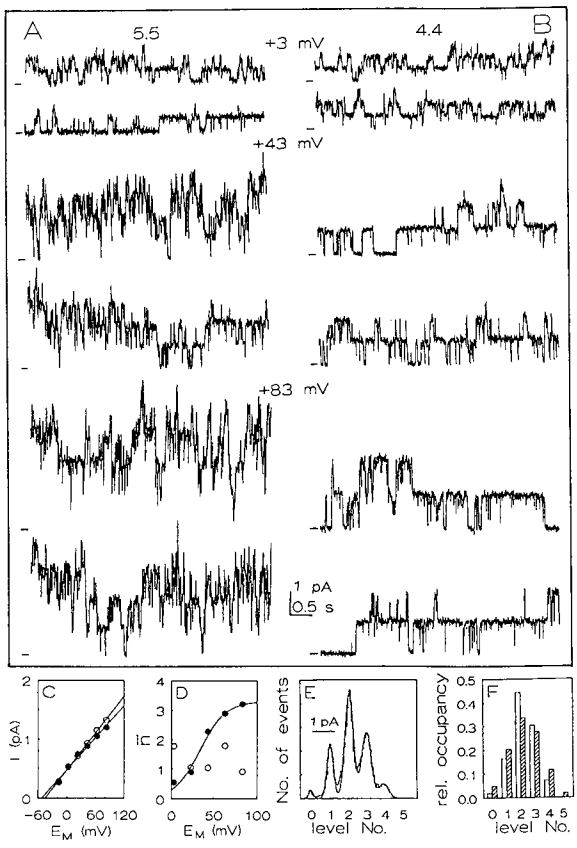

FIGURE 6. The effect of pH between 5.5 and 4.4 on single K_D channels in an outside-out patch. Representative single channel current traces at the indicated membrane potentials, and pH values. Upward deflection indicate channel opening and outward current. 0 current and no openings are indicated by a dash at the left of each record. Note the decrease in activity at the higher depolarizations between pH 5.5 (*A*) and 4.4 (*B*). Data filtered at 100 Hz, and sampled at 500 Hz. (*C*) Current-voltage (I-EM) relationship of the single channels of *A* and *B*. (*Symbols*) Average amplitude of unitary current jumps; ○: pH 4.4, ●: pH 5.5 (the SEM values are smaller than the symbol size). (*Line*) Linear regression fit to the data; the single channel conductance was 9.1 ± 0.6 at pH 5.5 and 10.5 ± 0.2 at pH 4.4. The respective reversal potentials were: −52.8 ± 8.6 and −45.1 ± 2.3 mV. (*D*) Voltage dependence of the average level occupancy, $\bar{n}$, calculated by $\bar{n} = \Sigma(iW_i)/\Sigma(W_i)$, where i denotes the level number, and W_i denotes the relative occupancy of the level i. (*Symbols*) $\bar{n}$ at pH 5.5 (●) and 4.4 (○). The line is a simple Boltzmann distribution, equivalent to Eq. 4, $\bar{n} = n_{max}/[1 + \exp(-z(E_M\text{-}E_0)F/RT)]$, fitted to data of pH 5.5, with the best-fit parameters z = 1.7 ± 0.4 and E_0 = 33.9 ± 4.1 mV, and the scaling factor, n_{max} = 3.3 ± 0.3 (±estimated error; R′ = 0.9000). (*E*) An amplitude histogram of 50 s current record at pH 5.5 at 43 mV, revealing equally spaced peaks (at least five identical channels were observed at this voltage, while maximum of six were observed at 63 mV). The reasonable fit of the Gaussian distribution to the histogram indicates that the filtering at 100 Hz does not affect significantly the estimate of the level probabilities. (*F*) Fitting binomial distribution (*hatched bars*) to observed probabilities of opening levels (*open bars*). With the number of noncorrelated observations estimated roughly as 12 (with the longest τ of gating of ~4 s; see Materials and Methods), the calculated χ^2 (0.23), indicates the high probability of the applicability of the binomial distribution ($P > 1\%$); and even if the number of noncorrelated observations is increased to 500 (the calculated χ^2 increasing to 9.45), $P > 5\%$.

insensitive before the patch excision, it is the decrease in N, the estimated number of available K_D channels in a cell, and not γ_s (Eq. 6), that accounts for the decrease in G_{max}, the voltage-independent component of the whole-cell conductance.

From the maximum conductance at pH 8.1, 5.3 nS, N in a whole cell was at least ~500. Given the average surface area of the protoplasts, of 865 mm^2, the average density of the channels was at least ~0.6 mm^{-2}. We would like to point out that these estimates are based on the assumption that the maximum probability of opening (P_o) was 1. An additional process that is voltage-independent in the time scale of our measurements, for example, slow inactivation (although no such inactivation has been observed as yet in *Vicia* K_D channels; Schroeder, 1988), could limit the maximum probability of opening of the channels during depolarization. Thus, the above value for N may be an underestimate of the true number of K_D channels in the whole cell membrane.

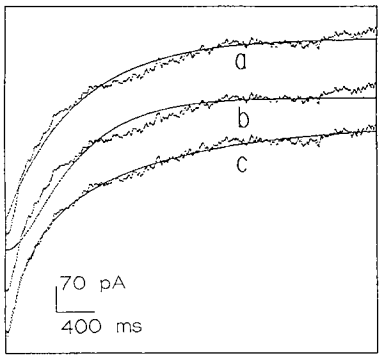

FIGURE 7. Macroscopic kinetics of activation of K_D channels. (*Noisy traces*) Currents elicited by stepping the membrane potential for 4 s from the holding potential of −87 mV to 63 mV, at pH 5.0. (*Smooth lines*) Currents calculated according to (*a*) C-O model ($A_0 + A_1 e^{-t/\tau}$; A_0 = 597, A_1 = −497, τ = 758 ms, R′ = .990); (*b*) classical Hodgkin-Huxley two-identical-independent-particle C-O model ($A_0 + A_1 [1 - e^{-t/\tau}]^2$; A_0 = 167, A_1 = 418, τ = 525 ms, R′ = .977) and (*c*) C-C-O model ($A_0 + A_1 e^{-t/\tau 1} + A_2 e^{-t/\tau 2}$; A_0 = 630, A_1 = −250, A_2 = −353, τ_1 = 211 ms, τ_2 = 1,295 ms, R′ = 0.997).

The Three-State Model of the K_D Channel Gating

We were unable to obtain patches with just one K_D channel, which would enable the direct determination of closing and opening rates. At best, we could estimate the average frequency of channel closing, i.e., β, by dividing the number of closing transitions by the time-channel integral (Ehrenstein et al., 1974). For example, in a 50 s record from the multichannel patch of Fig. 6 at pH 5.5 at 3 mV, β was ~7 s^{-1}. Therefore, and because of the irregularity in the single channel gating in the outside-side-out patches, to gain more insight into the effects of pH on gating, we chose to examine the gating model of the K_D channels using the kinetics of macroscopic relaxations. Fig. 7 illustrates a comparison of the time course of an activating whole-cell K_D current with predictions based on three types of models for channel gating: (*a*) a two-state (C-O) model of a single gating unit; (*b*) a two-identical-subunits model, in which each subunit independently undergoes C-O transitions, but both of them need to be in the O state for the channel to be open; (*c*) a sequential three-state model of a single gating subunit. The best fit was obtained with the three-state model.

In fitting the steady state conductance-voltage (G_K-E_M) relationship with the CCO model (Eq. 14), we used G_K/G_{max} as a measure of P_0 (Eq. 2), where G_{max} is the previously determined voltage-independent scaling factor of G_K (Eq. 4).

We fitted both τ's of activation and τ of deactivation (τ_d) vs E_M, simultaneously with G_K-E_M, with the appropriate functions (Eqs. 11–14). τ_d was fitted, rather arbitrarily (but see Figs. 8, *B* and *C*), along with the shorter time constant, τ_1. Before fit, to diminish variability, all data were normalized as described in Materials and Methods. The resulting parameters for pH 5.5 are listed in Table I. To compare with β derived previously from the single channel data from one well-behaved patch, of $\sim 7\ s^{-1}$, we calculated β from the Table I parameters (Eq. 11) for E_M of 26 mV (taking into account the 26 mV shift of the midpoint of activation between the two sets of data; see above), resulting in the value of $\sim 4\ s^{-1}$.

pH Effects on the CCO Model Parameters

Table I summarizes the parameters obtained from simultaneous fitting of the CCO model to G_K-E_M and τ's-E_M extracted from experiments conducted at 3 pH values, 8.1, 5.5, and 4.4, at which data were collected over sufficiently large voltage range.

TABLE I

The Effect of pH on the Parameters of the CCO Model for K_D Channels

pH	E_1	E_2	z_1	z_2	A_{21}	A_{o2}	B_1	B_2	z_1+z_2
	mV						s^{-1}		
8.1	53 ± 25	−42 ± 5	0.8 ± 0.3	1.4 ± 0.2	0.6 ± 0.2	1.0 ± 0.1	0.4 ± 0.03	1.2 ± 0.2	2.2
5.5	−36 ± 16	−2 ± 4	1.3 ± 0.9	1.3 ± 0.04	1.2 ± 0.9	0.9 ± 0.04	0.4 ± 0.02	1.7 ± 0.01	2.6
4.4	48 ± 25	−10 ± 4	0.7 ± 0.3	1.4 ± 0.3	0.8 ± 0.2	1.1 ± 0.2	0.4 ± 0.02	1.3 ± 0.2	2.1

G_K-E_M and t-E_M relationships, pooled separately at each pH (from 3, 8, and 4 cells at pH 8, 5.5, and 4.4, respectively), were fitted simultaneously with Eqs. 6–9. Listed are the best fit parameters (± estimated errors). The values of B_1 and B_2 were rescaled after the fitting using the scaling factors of τ's averaged at the different pH's. The "godness of fit" indicator, R', for the P_o-E_M data was 0.963, 0.973, and 0.919 for pH 4.4, 8.1 and 5.5, respectively; for the τ_1-E_M data R' was 0.807, 0.832, and 0.803, respectively; and for the τ_2-E_M data R' was 0.382, 0.314 and 0.077, respectively. See text for further details.

The total number of effective charges moved between the extreme conformations is at least 2, and it is pH independent (Table I). Irrespective of pH, three out of the four transition rates between the conformational states of the channel are, and remain, voltage dependent (roughly 1 to two effective charges are transfered upon each one of these transitions; Table I), whereas one -γ- is voltage independent (the effective charge transfered upon this transition, z_1-A_{21}, is not significantly different from 0 [Table I]).

In the range of pH 8.1–5.5–4.4, pH change did not affect significantly any of the other gating parameters, except E_2 and B_2 between pH 8.1 and 5.5 (with no further significant change between pH 5.5 and 4.4), and E_1 between pH 8.1 and 5.5, and again, between 5.5 and 4.4 (Table I). Fig. 8 illustrates the fit of the model to the data at the two extreme pH values: 4.4 and 8.1. Fig. 8*A* depicts the logarithmic dependence of the hypothesized transition rate constants α, β, γ, and δ on membrane potential at these pH values. The effect of protons between pH 8.1 and 4.4 is

reflected only in the simple shift of the characteristic voltage, E_2, by 32 ± 10 mV (± sum of error estimates of this parameter at the two pH's). This shift results in an increase of β, and in less pronounced changes in other rate constants, in particular, at a range of −20 to 80 mV, where the channels are active.

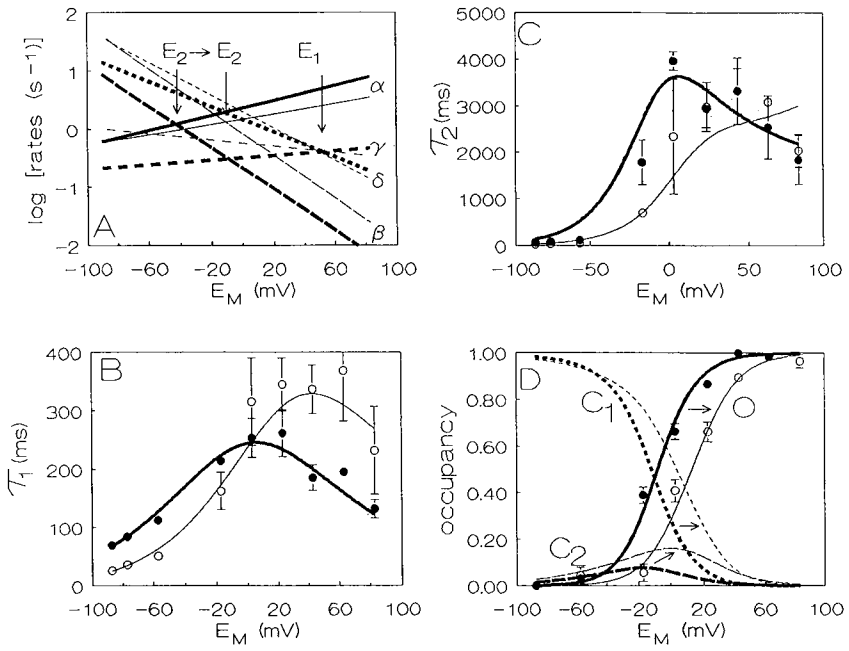

FIGURE 8. Fitting the CCO model simultaneously to G_K-E_M and $\tau - E_M$ relationships of the K_D channel at two pH values, denoted by symbols (data) and lines (calculated) as follows: 8.1: ●—● (n = 3); 4.4: O—O- n = 4); data are from a few of the cells of Fig. 3, as well as from a few additional cells. (*A*) Voltage dependence of transition rate constants, α, β, γ, δ, at the two pH's, calculated using Eq. 11 with parameters as in Table I. E_1, E_2: characteristic voltages of the transitions; horizontal arrow marks change upon acidification. (*B*) τ_1-E_M (*right*) and τ_d-E_M (*left*). Note the alignment of τ_1 and τ_d. (*Symbols*): Experimental values. (*Lines*) Eq. 12 with "+" preceding the square-root sign, with α, β, γ, δ. Note the shift between pH 8.1 and 4.4. (*C*) τ_2-E_M. Note the difference in range of values between τ_2 and τ_d. (*Symbols*) Experimental values. (*Lines*) Eq. 12 with "−" preceding the square-root sign, with the same α, β, γ, δ. (*D*) The pH and voltage dependence of the calculated occupancy, P (*lines*), of each of the three states, indicated in the Figure by O, C_1 and C_2. The respective P's were calculated as follows: P_0 from Eq. 13, $P_1 = 1/(1 + \gamma/\delta\ (1 + \alpha/\beta))$; $P_2 = 1 - (P_0 + P_1)$ (α, β, γ, δ are those depicted in Fig. 8 *A*). (*Symbols*) Experimental values of G_K normalized to G_{max} at the two pH values. Note that the calculated shifts of P_0 on the voltage axis represent more closely those of E_2 than of E_1.

These rate constants were used to reconstruct the fit to the data in Fig. 8, *B–D*. Fig. 8, *B* and *C*, depicts the effect of pH on the τ's of activation and deactivation. The deactivation and the smaller activation time-constant (τ_d and τ_1) are shifted by roughly 40 mV to more depolarized potentials as pH decreases from 8.1 to 4.4. This

shift explains the opposite effects of pH on $t_{1/2}$ at 63 mV vs τ_d at −87 mV (Fig. 3 *B*). The shift of the larger time constant (τ_2) does not appear to be significant due to the large scatter of data (Fig. 8 *C*).

Fig. 8 *D* illustrates the effect of pH on the distribution of the K_D channels between the three states at pH 4.4 and 8.1. The fit of the CCO model (*solid lines*) reconstructs the observed shift of P_o (*symbols*) by ~20 mV in the depolarized direction as pH decreases from 8.1 to 4.4. The calculated occupancies of states C_1 and C_2 shift similarly.

It should be noted here, that in spite of the significant shift of E_1 between pH 8.1 and 5.5 (by −88 ± 41 mV; ± sum of error estimates of this parameter at the two pH's), and a concomitant roughly 50-fold decrease in δ at pH 5.5, both the P_0-E_M (implicit in Fig. 3 *A*) and τ-E_M (not shown, but see Fig. 3 *B*) relationships at pH 5.5 are intermediate between those at pH 8.1 and 4.4, i.e., E_1 does not affect markedly the measured aspects of channel activation. This may be the source of the relatively large error in estimating this parameter.

DISCUSSION

Our goal is to elucidate the blocking effect of protons on the plant (guard cell) K_D channel current at the level of the mechanism of K_D channel activation. Because membrane depolarization is a major activator of this channel, we attempted to quantify the voltage dependence of gating, first by a simple two-state analysis (Boltzmann distribution, Eq. 4), then by a three-state analysis (Eqs. 11–14).

The voltage-independent properties of the K_D channel in *Vicia* protoplasts, i.e., relative ion selectivity, single-channel conductance (with the appropriate corrections for the experimental differences in concentrations), voltage sensitivity (i.e., z), and even the maximum current in a whole cell, are relatively uniform in the reports from different labs. Noteworthy, the same voltage sensitivity ($z = 2$) has been determined not only for the K_D channel in the intact cell (Blatt, 1991), but also for the classical delayed rectifier channel in the squid giant axon (Spires and Begenisich, 1992).

In contrast, the voltage-dependent properties of the K_D channel are not uniform. At comparable conditions of ion concentrations (of H^+, K^+ and Ca^{2+}), the most markedly varying parameter between the different reports about protoplasts is the half-activation voltage, E_0, including our own determinations at pH 5.5 for the macroscopic currents [7.7 ± 1.6 mV (mean ± SEM)] and for the single channel current in an excised patch (E_0 = 34 mV). From averaged data by Schroeder (1989; solutions identical to ours) which we refitted with Eq. 4, we estimated E_0 to be +11 mV, and from those of Fairley-Grenot and Assmann, +16 mV (1992; we estimated this shift based on the maximum and half-maximum chord conductances extracted from their published averaged data). Interestingly, in the intact cells (Blatt, 1988, 1990, 1991, 1992; E_0's estimated as before) the values of E_0 appear to vary between preparations, even with similar external solutions, between ~−10 and ~−50 mV. While in the intact cells, E_0 shift might reflect the shift in E_K (Moran, Iwasa, Ehrenstein, Mischke, Bare, and Satter, 1987; also see Blatt, 1991), the internal $[K^+]$ would have to vary roughly fivefold to account for the observed range of E_0, of ~40 mV. We tend to assume that the intact guard cells used in these experiments were

rather uniform in their turgor, therefore—also in their K^+ content. Thus, the variability of E_0, in protoplasts, as well as in intact cells, is suggestive of a labile cellular process governing the gating of the K_D channel. This may mean that occasionally, one or more of the negatively charged moieties that contribute to the electrical field sensed by the channel gates, is lost, for example, by dephosphorylation. The variability of E_0 (Fig. 4 *B*, for example) accounts, perhaps, for the relatively large scatter of voltage-dependent gating properties, such as the t's and τ's in our pooled data (Figs. 3 *B*, 8 *B* and *C;* see also Schroeder, 1989, Fig. 3). The fluctuations in $\bar{n}$ in the outside-out patch may be an extreme case of such lability. Interestingly, marked fluctuations in the opening probability were reported in reconstituted Ca-dependent K channels undergoing phosphorylation-dephosphorylation cycles (Chung, Reinhart, Martin, Brautigan, and Levitan, 1991).

The CCO Model Description of K_D Channels in Vicia

The steady state current scaling factor, G_{max}, and the total effective charge of gating, z, could be approximated relatively closely by a simple Boltzmann analysis (Eq. 4). However, more detailed modeling was required to fit all of our data, including the kinetics of current activation (Fig. 7). Thus, we described the macroscopic activation-deactivation of the K_D channel type in *Vicia* protoplasts in terms of a sequential, three-state model (CCO), with four voltage-dependent rate constants for transitions between the states. A Hodgkin-Huxley-type 2-independent-subunits (HH) model, has been suggested for the description of this channel, based on analysis of <1 s long current traces (Schroeder, 1989). We found that the CCO model fits 5 s long K_D current traces better. Because the HH model is mathematically equivalent also to a linear three-state CCO model (Armstrong, 1969), in which $\beta = 2\delta$, and $\gamma = 2\alpha$, our approach consists, in fact, of adding four additional independent parameters.

The three-state model allows insight into the intermediate steps of K_D channel gating: it appears that while the transitions into and out of the open state are similarly voltage dependent, most of the voltage dependence between the two closed states resides in the rate constant δ of the transition back to the far closed state.

It is important to note here that the CCO model for the K_D channel is a reduced model (see also Schroeder, 1989). Single-channel open and closed times, in the range of 20 and 1 ms, respectively (Hosoi, Iino, and, Shimazaki, 1988), reveal another time scale of gating. However, as a larger number of parameters would yield the fitting procedure impractical, in our macroscopic experiments, this fast time scale was filtered out. If, for example, in this reduced CCO model, the O state actually represents a burst of channel openings rather than individual channel openings (i.e., an additional lumped $C_0 \leftrightarrow O_{true}$ transition), then the rate constant β should predict the inverse of burst duration. Indeed, the value of such β (average frequency of closings determined from one patch, in a record filtered at 20 Hz) was comparable to an average value of β calculated for equivalent conditions from whole-cell data. This supports the notion that our analysis of whole cell currents may have relevance to the single channel behavior. Using our reduced model, we aimed to resolve the extracellular pH effects on the transition rates of the channel on a time scale extending roughly between 50 to 5,000 ms.

The Mechanism of pH Blocking Action

In *Vicia* protoplasts, extracellular protons exert a major inhibitory effect on the macroscopic conductance of the K_D channel. We ascribe these effects of protons solely to the *external* surface of the membrane, due to the efficient buffering of the internal solution (Marty and Neher, 1983). Over most of the voltage range examined (> -20 mV), the steady state whole-cell K_D conductance in protoplasts decreased by $\sim 75\%$ with acidification between 8.1 and 4.4 (Fig. 3). An essentially similar effect ($\sim 25\%$ decrease at pH range 7.4–5.5) has been reported for guard cells in situ (Blatt, 1992).

What is the mechanism of these effects on conductance? Do protons change the electrical interactions of the channel and thus the gating (an effect on P_0 and on τ) by altering: (*a*) the effective charges of the gating particles (an effect on z); and (*b*) the surface charge near the channel (an effect on E_0)?

Do protons affect the voltage-independent parameters of the channels (G_{max}) by: (*a*) blocking partially the open channel (an effect on γ_s); and (*b*) knocking out channels from the membrane or modulating their availability for opening by depolarization (an effect on N)?

Our answers are based on the results from both of our approaches: the two-state and the three-state modeling. Fig. 4 *C* and Table I reveal that external protons do not alter significantly the voltage sensitivity (i.e., the effective charges) of the K_D channel gating particles.

In contrast, protons do modify the electrical field sensed by the gates, as evident from the shifts of the voltage-dependent properties (P_0, τ's) along the voltage axis (Figs. 4 *B*, 8 *B–D*).

The Negative Surface Charge Near the K_D Channel

These pH-dependent shifts suggest that protons decrease the negative surface charge density at the external surface of the membrane, in the vicinity of the K_D channel gates.

The slope of E_0-pH (Fig. 4 *B*) is indicative (in a complicated way) of the density of such titratable charges (Gilbert and Ehrenstein, 1969, 1970). Thus, it may be of interest to compare such observed shifts and calculated surface charge spacing for the delayed rectifier K channel between various preparations: at pH range 4–6.5, in the axon membrane of the marine worm *Myxicola,* the slope was -9.3 mV/pH unit (Schauf and Davies, 1976), and the average spacing between charges, d_t, was ~ 13 Å (Begenisich, 1975; Schauf, 1975); in the giant axon of the squid the slope was -18.7 mV/pH unit and d_t was 8 A (Carbone, Fioravanti, Prestipino, and Wanke, 1978), in the frog node the slope was -49 mV/pH (Druin and The, 1969) and d_t was 20 Å (Mozhayeva and Naumov, 1970), and at a pH range 4.4 to 8.1, in *Vicia* protoplasts the slope was -6.2 mV/pH unit (Fig. 4 *B*). Given the much lower ionic strength of the external medium in our experiments (see Materials and Methods), as compared to the above examples, the small slope in *Vicia* would be consistent with a lower surface charge density (and larger spacing). Indeed, we estimated the average spacing between the negative charges in the vicinity of the K_D channel gates *in Vicia* as 39 Å, considerably larger than in the above examples. (In an interesting contrast to

the animal K channel, recent analysis of external surface charge near a neuronal Ca channel reveals their large spacing: ~33 Å [Becchetti et al., 1992]). A possible interpretation of these differences may be that those parts of the channel protein that contribute to the negative surface charge in the animal K channel (reviewed by Hille, 1992), are different in the K_D channel in the plant cell protoplast.

The above considerations are only rough approximations: the effects of protons on the gating properties of the K_D channel are only partially consistent with a simple titration of surface charges. We note a departure from a homogeneous shift of voltage-dependent properties along the voltage axis (for example: between pH 8.1 and 4.4 P_0 shifts by ~20 mV (Fig. 8 *D*), while τ_1 shifts by ~40 mV, furthermore, τ_1 increases [Fig. 8 *C*]). This, by itself, does not necessarily contradict the surface charge theory (Gilbert and Ehrenstein, 1984). However, even the more elementary parameters are affected differently: E_1 and E_2 do not shift similarly with changes of pH (Table I). Moreover, the shift of E_1 is not a monotonic function of pH (Table I). Therefore, it is unlikely that protons affect simply the external surface charge of the membrane. Rather, we may interpret this effect as that of protonation of discrete negative charges, perhaps even more than one class of sites, in the local environment of the gating subunit, resulting in different electrical fields sensed during the two conformational transitions (see also Gilbert and Ehrenstein, 1984). If applicable, the approximate pK_{sc} of this protonation, derived from our data within the framework of the simple surface charge theory, is 4.8, corresponding to the bulk pH (i.e., apparent pK_{sc}) of 5.0. Finally, it may be of interest to note that the pK_{sc} of the negative surface charge site near the neuronal Na channel of the frog was 4.6 (this corresponds to bulk pH of 5.3; Gilbert and Ehrenstein, 1970), and that near the cardiac Na channel was 5.16 (Zhang and Siegelbaum, 1991).

A Separate Effect of pH on G_{max}?

The shift in P_0-E_M accounts for part of the observed decrease of the steady state conductance with acidification (Fig. 3 *A*). In addition to this effect on the voltage-dependent gating parameters, acidification decreases also the voltage-independent property, G_{max}, i.e., the product $N\gamma_s$ (Eq. 6). Because single channel conductance, γ_s, is hardly affected by pH change, the decrease of macroscopic conductance should be attributed to the diminished number of available channels, N, due to protonation. Actually, this is paramount with redefining N as the product of the true number of K_D channels in the membrane and an additional voltage-independent availability factor, representing, in this case, the effect of protonation on channel gating. Indeed, the effect of protonation on N, extracted by binomial analysis of single channel records from two excised, outside-out patches, is consistent with this conclusion (in spite of the irregularity of gating). Postulating such a single protonation site modifying the voltage-independent aspect of K_D channel gating, its pK_a has been estimated as 4.8 ± 0.3 (±estimates of standard error; $n = 6$). However, if the data at pH 8.1 are excluded from the fit, pK_a is 4.6 ± 0.1 ($n = 5$; Fig. 4 *A*). Indeed, the relatively large jump in G_{max} between pH 8 and 7.5 suggests an additional protonation site (perhaps similar to that with pK_a of 9.2 suggested by Mozhayeva and Naumov [1970] for the frog node K channel), but extention of experiments beyond pH 8 is required to substantiate this here. Thus the pk_a 4.8 may be interpreted as reflecting a lumped

site rather than a truly single site. For comparison, the delayed rectifier channel in frog myelinated nerve was also blocked by extracellular protons, with a pK_a of 4.6 (Druin and The, 1969) or 4.4 (Hille, 1973). In *Myxicola,* the pK_a for G_K inhibition was also 4.4 (Schauf and Davis, 1976), but in the crayfish it was 6.3 (Schrager, 1974). In the Na channels in the frog nerve, the blocking protonation site had a pK_a of 4.8 (Woodhull, 1973).

In conclusion, in the physiological range of external pH, the plant K_D channel availability for activation (N) may be governed by a site similar to that in K channels in animal membranes. This might be a carboxyl side chain group of the channel protein itself, slightly modified by its local environment (Schauf and Davis, 1976). The protonation of such a local discrete negative charge may lead to the compound observed effects of acidification (Gilbert and Ehrenstein, 1984; Zhang and Siegelbaum, 1991). Is then the site that governs N, the voltage-independent channel availability, separate from the site that affects the local electrical fields sensed by the gating moieties? Further experiments are needed to resolve this question.

Physiological Significance

The modulatory effects of pH on K_D channels are consistent with the physiological requirements for their function. At the apoplastic pH of ~5, prevailing when the stomatal guard cells swell and stomata open (Edwards et al., 1988), acidification might aid the closing of the K_D channels by hyperpolarization. While hyperpolarization alone would be sufficient to close the K_D channels in this instance, membrane potential could be subject to a separate modification by changes in the relative permeabilities to different ions (for example, depolarization brought about by an increase in permeability to Ca^{2+}, or Cl^-). In such a case, extracellular protons might act as an additional gating element preventing the loss of intracellular K^+. At the higher apoplastic pH, prevailing when the stomata normally close (Edwards et al., 1988), most of the K_D channels will be able to serve as the pathway for K^+ efflux, when the membrane becomes depolarized. Apoplastic pH changes, together with the plant hormone, Abscisic acid (ABA), have been suggested to act as signals of the decrease in water availability, during which stomata close (Gollan, Schurr, and Schulze, 1992). For example, increased apoplastic pH appears to be correlated with drought stress conditions imposed either by pressure dehydration of detached leaves (Hartung, Radin, and Hendrix, 1988), or by soil dehydration (Gollan et al., 1992). The enhanced activity of the K_D channels in guard cells at such conditions would be of beneficial value, since it would promote stomata closure and preserve the plant water potential.

Thanks are due to Ms. A. Ben David for help in protoplast isolation and to Dr. H. Jarosch for help with the SAS and Fortran fitting routines. The authors are grateful to Drs. I. Steinberg, G. Ehrenstein, K. Iwasa, Y. Palti, and S. Assmann for helpful comments on an earlier version of the manuscript and to Dr. Blatt for making his paper available to us before we could see it published.

This research was supported by the US-Israel Binational Science Foundation grant No. 89-00235 to A. Schwartz by the US-Israel Binational Agricultural Research and Development Fund grant No. 91-00293 to N. Moran and the Basic Research Foundation grant No 487/89 from The Israel Academy of Sciences and Humanities to N. Moran.

Original version received 29 September 1992 and accepted version received 9 December 1993.

REFERENCES

Anderson, J. A., S. S. Huprikar, L. V. Kochian, W. J. Lucas, and R. F. Gaber. 1992. Functional expression of a probable *Arabidopsis thaliana* potassium channel in *Saccharomyces cerevisiae*. *Proceedings of the National Academy of Sciences, USA*. 89:3736–3740.

Armstrong, C. M. 1969. Inactivation of the potassium conductance and related phenomena caused by quaternary ammonium ion injection in squid axons. *Journal of General Physiology*. 54:553–575.

Assmann, S. M., N. Moran, and A. Schwartz. 1988. Whole-cell K^+ currents in guard cell protoplasts of *Vicia Faba* and *Commelina communis*. *Plant Physiology*. 86:83 (Abstr.)

Assman, S. M., L. Simoncini, and J. Schroeder. 1985. Blue light activates electrogenic ion pumping in guard cell protoplasts of *Vicia faba*. *Nature*. 318:285–287.

Balser, J. R., D. M. Roden, and P. B. Bennett. 1990. Global parameter optimization for cardiac potassium channel gating models. *Biophysical Journal*. 57:433–444.

Becchetti, A., A. Arcangeli, M. R. Del Bene, M. Olivotto, and E. Wanke. 1992. Intra and extracellular surface charges near Ca^{2+} channels in neurons and neuroblastoma cells. *Biophysical Journal*. 63:954–965.

Begenisich, T. 1975. Magnitude and location of surface charges in *Myxicola* giant axons. *Journal of General Physiology*. 66:47–65.

Begenisich, T., and M. Danko. 1983. Hydrogen ion block of the sodium pore in squid giant axons. *Journal of General Physiology*. 82:599–618.

Behrens, M. I., A. Oberhauser, F. Bezanilla, and R. Latorre. 1989. Batrachotoxin-modified sodium channels from squid optic nerve in planar bilayers. *Journal of General Physiology*. 93:23–41.

Bertl, A., H. G. Klieber, and D. Gradmann. 1988. Slow kinetics of a potassium channel in *Acetabularia*. *Journal of Membrane Biology*. 102:141–152.

Blatt, M. R. 1988. Potassium-dependent, bipolar gating of K^+ channels in guard cells. *Journal of Membrane Biology*. 102:235–246.

Blatt, M. R. 1990. Potassium channel currents in intact stomatal guard cells: rapid enhancement by abscisic acid. *Planta*. 180:445–455.

Blatt, M. R. 1991. Ion channel gating in plants: physiological implications and integration for stomatal function. *Journal of Membrane Biology*. 124:95–112.

Blatt, M. R. 1992. K^+ channels of stomatal guard cells: characteristics of the inward rectifier and its control by pH. *Journal of General Physiology*. 99:615–644.

Cao, Y., M. Anderova, N. M. Crawford, J. I. Scroeder. 1992. Expression of an outward-rectifying potassium channel from maize mRNA and complementary RNA in *Xenopus* oocytes. *Plant Cell*. 4:961–969.

Carbone, E., R. Fioravanti, G. Prestipino, and E. Wanke. 1978. Action of extracellular pH on Na^+ and K^+ membrane currents in the giant axon of *Loligo vulgaris*. *Journal of Membrane Biology*. 43:295–315.

Chung, S., P. H. Reinhart, B. L. Martin, D. Brautigan, and I. B. Levitan. 1991. Protein kinase activity closely associated with a reconstituted calcium-activated potassium channel. *Science*. 253:560–562.

Draber, S., R. Schultze, and U-P. Hansen. 1993. Cooperative behavior of K^+ channels in the tonoplast of *Chara corallina*. *Biophysical Journal*. 65:1553–1559.

Druin, H., and R. The. 1969. The effect of reducing extracellular pH on the membrane currents of the Ranvier node. *Pfluegers Archives*. 313:80–88.

Edwards, M. C., G. N. Smith, and D. J. F. Bowling. 1988. Guard cells extrude protons prior to stomatal opening. A study using fluorescence microscopy and pH micro-electrode. *Journal of Experimental Botany*. 39:1541–1547.

Ehrenstein, G., R. Blumenthal, R. Latorre, and H. Lecar. 1974. Kinetics of the opening and closing of individual excitability-inducing material channels in a lipid bilayer. *Journal of General Physiology.* 63:707–721.

Fairley-Grenot, K. A., and S. M. Assmann. 1992. Whole-cell K^+ current across the plasma membrane of guard cells from a grass: *Zea mays*. *Planta.* 186:282–293.

Gilbert, D. L., and G. Ehrenstein. 1969. Effect of divalent cations on potassium conductance of squid axons: determination of surface charge. *Biophysical Journal.* 9:447–463.

Gilbert, D. L., and G. Ehrenstein. 1970. Use of a fixed charge model to determine the pK of the negative sites on the external membrane surface. *Journal of General Physiology.* 55:822–825.

Gilbert, D. L., and G. Ehrenstein. 1984. Membrane surface charge. *Current Topics in Membrane Transport.* 22:407–421.

Gill, R. E., and W. Murray. 1978. Algorithms for the solution of non-linear least squares problems. *Society of Industrial and Applied Mathematics Journal.* 15:977–992.

Gollan, T., U. Schurr, and E. D. Schulze. 1992. Stomatal response to drying soil in relation to changes in the xylem sap composition of *Helianthus Annuus* I. The concentration of cations, anions, amino acids in, and pH of, the xylem sap. *Plant Cell and Environment.* 15:551–559.

Grahame, D. C. 1947. The electrical double layer and the theory of electrocapilarity. *Chemical Reviews.* 41:441–501.

Hagiwara, S., S. Miyazaki, M. W. Moody, and J. Patlak. 1978. Blocking effects of barium and hydrogen ions on the potassium current during anomalous rectification in the starfish egg. *Journal of Physiology.* 279:167–185.

Hamill, O. P., A. Marty, E. Neher, B. Sakmann, and F. Sigworth. 1981. Improved patch-clamp techniques for high-resolution current recording from cells and cell-free membrane patches. *Pfluegers Archives.* 391:85–100.

Hanke, W., and C. Miller. 1983. Single chloride channels from *Torpedo* electroplax: activation by protons. *Journal of General Physiology.* 82:25–45.

Hartung, W., J. W. Radin, and D. L. Hendrix. 1988. Abscisic acid movement into the apoplastic solution of water stressed cotton leaves: role of apoplastic pH. *Plant Physiology.* 86:908–913.

Hedrich, R., and J. I. Schroeder. 1989. The physiology of ion channels and electrogenic pumps in higher plants. *Annual Review of Plant Physiology.* 40:539–569.

Hille, B. 1973. Potassium channels in myelinated nerve: selective permeability to small cations. *Journal of General Physiology.* 61:669–686.

Hille, B. 1992. Ionic Channels of Excitable Membranes. Sinauer Associates, Inc., Sunderland, MA. 525–544.

Hodgkin, A. I., and A. F. Huxley. 1952. A quantitative description of membrane current and its application to conduction and excitation in nerve. *Journal of Physiology.* 117:500–544.

Hosoi, S., M. Iino, and K. I. Shimazaki. 1988. Outward-rectifying K^+ channels in stomatal guard cell protoplasts. *Plant and Cell Physiology.* 29:907–911.

Huang, L. Y. M., W. A. Catterall, and G. Ehrenstein. 1978. Selectivity of cations and nonelectrolytes for acetylcholine-activated channels in cultured muscle cells. *Journal of General Physiology.* 71:397–410.

Huang, L. Y. M., N. Moran, and G. Ehrenstein. 1984. Gating kinetics of batrachotoxin-modified sodium channels in neuroblastoma cells determined from single-channel measurements. *Biophysical Journal.* 45:313–322.

Ilan, N., A. Schwartz, and N. Moran. 1991. pH effect on K^+ channels in plasmalemma of guard cell protoplasts. *Plant Physiology.* 96:137*a*. (Abstr.)

Ilan, N., A. Schwartz, and N. Moran. 1992. Proton block of K channels in plasma membrane of guard cell protoplasts: a patch-clamp study. *In* Ninth International Workshop on Plant Membrane Biology, Monterey, CA. 30*a*. (Abstr.)

Iwasa, K., G. Ehrenstein, N. Moran, and M. Jia. 1986. Evidence for interactions between batrachotoxin-modified channels in hybrid neuroblastoma cells. *Biophysical Journal* 50:531–537.

Ketchum, K. A., A. Shrier, and R. J. Poole. 1989. Characterization of potassium-dependent currents in protoplasts of corn suspension cells. *Plant Physiology.* 89:1184–1192.

Kruse, T., G. Tallman, and E. Zeiger. 1989. Isolation of guard cell protoplasts from mechanically prepared epidermis of *Vicia faba* leaves. *Plant Physiology.* 90:1382–1386.

Lee, Y., and R. L. Satter. 1989. Effects of white, blue, red light and darkness on pH of the apoplast in *Samanea* pulvinus. *Planta* 178:31–40.

MacRobbie, E. A. C. 1987. Ionic relations in guard cells. *In* Stomatal Function. E. Zeiger, G. D. Farquhar, and I. R. Cowan, editors. Stanford University Press, Stanford, CA 125–162.

Marty, A., and E. Neher. 1983. Tight seal whole-cell recording. *In* Single Channel Recording. B. Sakmann and E. Neher, editors. Plenum Publishing Corp., NY. 107–121.

Moran, N., G. Ehrenstein, K. Iwasa, C. Bare, and C. Mischke. 1986. Ion channels in plant cell protoplasts. *In* Ionic Channels in Cells and Model Systems. R. Latorre, editor. Plenum Publishing Corp., NY 195–205.

Moran, N., G. Ehrenstein, K. Iwasa, C. Mischke, and R. L. Satter. 1988. Potassium channels in motor cells of *Samanea saman:* a patch-clamp study. *Plant Physiology.* 88:643–648.

Moran, N., D. Fox, and R. L. Satter. 1990. Interaction of the depolarization-activated K^+ channel of *Samanea saman* with inorganic ions: a patch-clamp study. *Plant Physiology.* 94:424–431.

Moran, N., K. Iwasa, G. Ehrenstein, C. Mischke, C. Bare, and R. L. Satter. 1987. Effects of external K^+ on K channels in *Samanea* protoplasts. *Plant Physiology.* 83:112S. (Abstr.)

Moran, N., and R. L. Satter. 1989. K^+ channels in plasmalemma of motor cells of *Samanea saman. In* Plant Membrane Transport. J. E. A. Dainty, editor. Elsevier Science BV, Amsterdam. 529–530.

Mozhayeva, G. N., and A. P. Naumov. 1970. Effect of surface charge on the steady-state potassium conductance of nodal membrane. *Nature.* 228:164–166.

Outlaw, W. H. 1983. Current concepts on the role of potassium in stomatal movements. *Physiologia Plantarum.* 59:302–311.

Raschke, K., and G. D. Humble. 1973. No uptake of anions required by opening stomata of *Vicia faba:* Guard cells release hydrogen ions. *Planta.* 115:47–57.

Robinson, R. A., and R. H. Stokes. 1965. Electrolyte Solutions. Butterworths, London. 481 pp.

Sanders, D. 1990. Kinetic modeling of plant and fungal membrane transport systems. *Annual Review of Plant Physiology and Plant Molecular Biology.* 41:77–107.

Schachtman, D. P., J. L. Schroeder, W. J. Lucas, J. A. Anderson, R. F. Gaber. 1992. Expression of an inward-rectifying potassium channel by the *Arabidopsis* KAT1 cDNA. *Science.* 258:1654–1658.

Schauf, C. L. 1975. The interactions of calcium with with *Myxicola* giant axons and a description in terms of a simple surface charge model. *Journal of Physiology.* 248:613–624.

Schauf, C. L., and K. J. Wilson. 1987. Effects of abscisic acid on K^+ channels in *Vicia faba* guard cell protoplasts. *Biochemical and Biophysical Research Communication.* 145:284–290.

Schauf, C. L., and F. A. Davis. 1976. Sensitivity of the sodium and potassium channels of *Myxicola* giant axons to changes in external pH. *Journal of General Physiology.* 67:185–195.

Schrager, P. 1974. Ionic conductance changes in voltage clamped crayfish axons at low pH. *Journal of General Physiology.* 64:666–690.

Schroeder, J. I. 1988. Potassium transport properties of potassium channels in the plasma membrane of *Vicia faba* guard cells. *Journal of General Physiology.* 92:667–683.

Schroeder, J. I. 1989. Quantitative analysis of outward rectifying K^+ channel currents in guard cell protoplasts from *Vicia faba*. *Journal of Membrane Biology*. 107:229–235.

Schroeder, J. I., K. Raschke, and E. Neher. 1987. Voltage dependence of K^+ channels in guard cell protoplasts. *Proceedings of the National Academy of Sciences, USA*. 84:4108–4112.

Sentenac, H., N. Bonneaud, M. Minet, F. Lacroute, J.-M. Salmon, F. Gaymard, and C. Grignon. 1992. Cloning and expression in yeast of a plant potassium ion transport system. *Science*. 256:663–665.

Shimazaki, K., M. Iino, and E. Zeiger. 1986. Blue light-dependent proton extrusion by guard-cell protoplasts of *Vicia faba*. *Nature* 319:324–326.

Spanswick, R. M. 1981. Electrogenic ion pumps. *Annual Review of Plant Physiology*. 32:267–289.

Spires, S., and T. Begenisich. 1992. Modification of potassium channel kinetics by amino group reagents. *Journal of General Physiology*. 99:109–129.

Starrach, N., and W.-E. Mayer. 1989. Changes of the apoplastic pH and K^+ concentration in the *Phaseolus* pulvinus in situ in relation to rhythmic leaf movements. *Journal of Experimental Botany*. 40:865–873.

Tester, M. 1990. Plant ion channels: whole-cell and single-channel studies. *New Phytology*. 114:305–340. (Tansley Review No. 21.)

Ueno, S., T. Nakaye, and N. Akaike. 1992. Proton-induced sodium current in freshly dissociated hypothalamic neurones of the rat. *Journal of Physiology*. 447:309–327.

Van Duijn, B. 1993. Hodgkin-Huxley analysis of whole-cell outward rectifying K^+ currents in protoplasts from tobacco cell suspension cultures. *Journal of Membrane Biology*. 132:77–85.

Woodhull, A. M. 1973. Ionic blockage of sodium channels in nerve. *Journal of General Physiology*. 61:687–708.

Zeiger, E. 1983. The biology of stomatal guard cells. *Annual Review of Plant Physiology*. 34:441–475.

Zhang, J. F., and S. A. Siegelbaum. 1991. Effects of external protons on single cardiac sodium channels from guinea pig ventricular myocytes. *Journal of General Physiology*. 98:1065–1083.